

11. Gravitational Lensing.

11.1. Some History

The first publication on the gravitational deflection of light appeared in 1804 in Germany: “Die Ablenkung eines Lichtstrahlsdurch die Attraktion eines Weltkörpers...” by the geodesist and astronomer Johann Soldner who calculated the deflection at the solar limb to be $\phi = 0,84$ arcsec. This is actually the same value obtained more than 100 years later by Einstein (1911) who didn't know of the paper of Soldner. In lect. 01 we derived this same value

$$\alpha(Newton) = \frac{2GM}{c^2 r} \quad (11.1)$$

using Newton's mechanics and the quantum property of light. Einstein's request to measure the deflection by the sun was soon followed by astronomers. An expedition travelled in 1914 to Russia in an attempt to observe a total solar eclipse on the Crimian Peninsula. Sadly enough during their preparations World War I broke out and the group members were captured by Russian Soldiers. These unfortunate circumstances were however fortunate for Einstein himself. After he completed his General Relativity he could show that the deflection angle in his new theory was actually twice the formerly published value

$$\alpha(Einstein) = \frac{4GM}{c^2 r} \quad (11.2)$$

As mentioned in lect.01 Arthur Eddington and his team in 1919 were able to measure the deflection during two observations of a total eclipse and could confirm the correct value predicted by Einstein within an error of 20%. This accordance of observations with the new theory was widely spread by the international press and established Einstein's reputation and popularity. There was little further progress in the next four decades. Besides some further theoretical papers no new observations were published. Einstein himself reported in 1936 about the appearance of a luminous circle when a stellar source and lens are exactly aligned, a constellation today called an *Einstein ring*. In the sixties of the past century gravitational lensing was studied more frequently by theorists. At last in 1979 the first double quasar was discovered with the HST by Walsh who was also able to confirm conclusively the existence of a gravitational lens. Since this time the field began to boom and attracted more and more scientists. In the last two decades gravitational lensing matured to an important tool of modern astronomy. It proved especially useful for the study of dark matter, i.e. matter which does not show up in optical surveys, but its existence is verified by its gravitation.

11.2. Light bending in Schwarzschild metric.

The expression (11.2) is the basis of weak gravitational lensing. Therefore we will first analyse light bending in Schwarzschild metric starting with expressions of lect. 3. The specific angular momentum was given in equ. (3.20)

$$j = r^2 \dot{\phi} \quad (11.3)$$

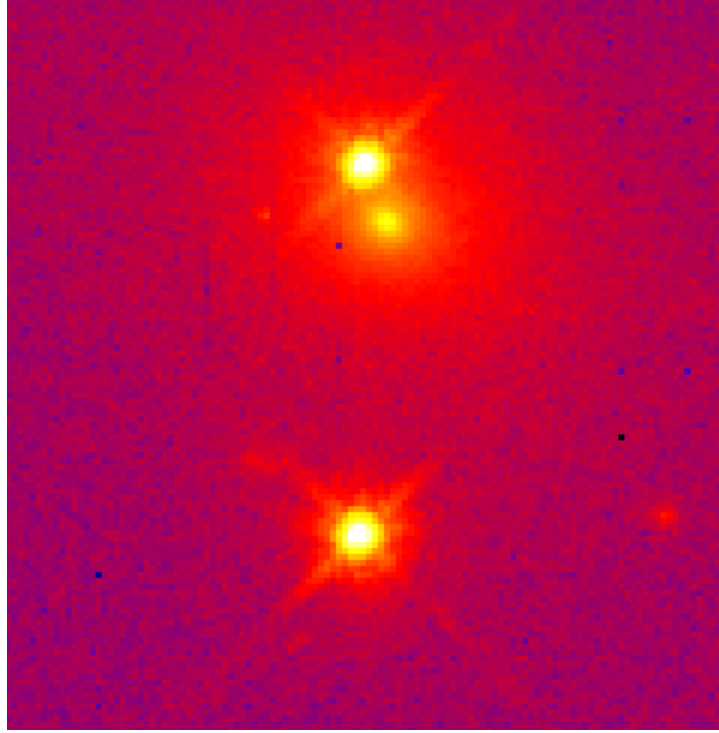


Fig. 11.1. A false color HST image of the first lens: Double quasar Q0957+561. Image A at the bottom, image B at the top, they are separated by $6''.1$. Slightly below B part of the lensing galaxy is visible. Image B has only $1''$ distance from the galaxy and is seen through their halo. Credits: E.E. Falco et al. (CASTLE collaboration [47]) and NASA.) from W. Wambsganss, Living Reviews in Relativity (1998-12).

and the energy and effective potential for massless particles equ. (3.40). We divide by j , set the impact parameter $b = \frac{j}{\varepsilon}$ as in lect. 03 and rescale $rj \rightarrow r$

$$\dot{r}^2 = \varepsilon^2 - \frac{j^2}{r^2} \left(1 - \frac{r_s}{r} \right) \rightarrow \dot{r}^2 = \frac{1}{b^2} - \frac{1}{r^3} (r - r_s) \quad (11.4)$$

In order to derive an analytic expression for a specific orbit, e.g. a null geodesic, we need

$\frac{d\varphi}{dr} = \frac{d\varphi}{d\tau} / \frac{dr}{d\tau}$. For this purpose we divide \dot{r} by $\frac{d\varphi}{d\tau} = \frac{j}{r^2}$. We obtain

$$\frac{d\varphi}{dr} = \frac{1}{r^2} \left(\frac{1}{b^2} - \frac{1}{r^3} (r - r_s) \right)^{-1/2} \quad (11.5)$$

or

$$\frac{d\varphi}{dr} = \frac{1}{\left(r^4 b^{-2} - r[r - r_s] \right)^{1/2}} \quad (11.6)$$

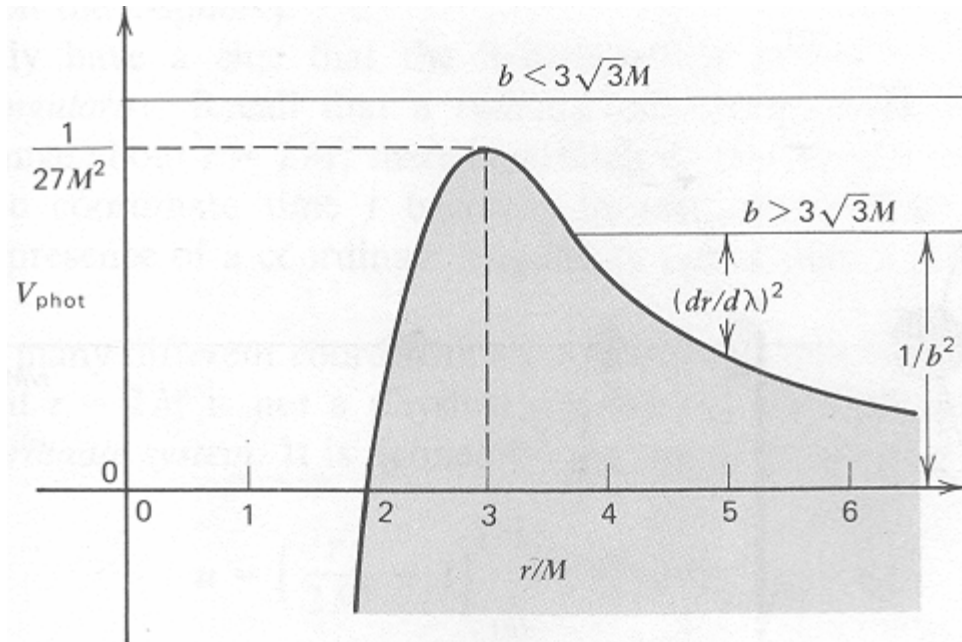


Fig. 11.2. This figure was already used in lect. 3. Unbound orbits are those with $b^2 > 27M^2 = 27\frac{r_s^2}{4}$. Credit: St.L. Shapiro and S.A. Teukolsky

An unbound orbit is a hyperbola. The angular difference $\Delta\varphi = \varphi(+\infty) - \varphi(-\infty)$ is the quantity which we ask for to describe the light bending observations.

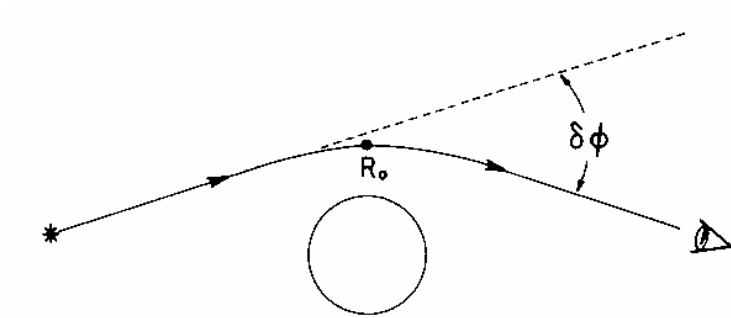


Fig. 11.3. The hyperbolic orbit near a mass. At $r = R_0$ we have $\dot{r} = 0$ and $V(R_0) = E^2/2$. Credit: R.M. Wald

With the turning point condition $\dot{r} = 0$ we obtain from (11.4)

$$1 - \frac{b^2}{r^3}(r - r_s) = 0 \quad (11.7)$$

and for $r = R_0$

$$R_0^3 - b^2(R_0 - r_s) = 0 \quad (11.8)$$

The largest root is

$$R_0 = \frac{2b}{3^{1/2}} \cos \left[\frac{1}{3} \cos^{-1} \left(-\frac{3^{3/2} r_s}{2b} \right) \right] \quad (11.9)$$

We obtain the angular difference (s.fig.11.3) by integrating (11.6)

$$\Delta\varphi = 2 \int_{R_0}^{\infty} \frac{dr}{\left(r^4 b^{-2} - r[r - r_s] \right)^{1/2}} \quad (11.10)$$

Note that the integration goes from $R_0 \rightarrow \infty$ which yields only half of the angular difference $\Delta\varphi$ therefore we multiply the integral by a factor 2. It is convenient to change variables

$$u = \frac{1}{r} \text{ and } du = -\frac{dr}{r^2} \quad (11.11)$$

With this transformation (11.8) becomes

$$\Delta\varphi = 2 \int_{0_0}^{1/R_0} \frac{du}{\left(b^{-2} - u[u - u^2 r_s] \right)^{1/2}} \quad (11.12)$$

In flat space $2M = r_s = 0$ and from (11.6) we find $R_0 = b$. In this case (11.10) gives

$$\Delta\varphi|_{M=0} = 2 \sin^{-1}(b/R_0) = 2 \sin^{-1}(1) = \pi \quad (11.13)$$

which describes a straight line. The solution for $M \neq 0$ must deviate from a straight and give a non vanishing contribution. We use (11.6) to eliminate b in (11.10) with

$$b^2 = \frac{R_0^3}{R_0 - r_s} \quad (11.14)$$

We write the integral in the form

$$\Delta\varphi = 2 \int_{0_0}^{1/R_0} \frac{du}{\left(R_0^{-2} - r_s R_0^{-3} - u^2 + u^3 r_s \right)^{1/2}} \quad (11.15)$$

We ask for the difference $\Delta\varphi$ when the mass is changed by ΔM . R_0 is kept fixed and we obtain the first order Taylor coefficient as

$$\begin{aligned} \frac{\partial(\Delta\varphi)}{\partial M}\Big|_{M=0} &= 2 \int_0^{1/R_0} \frac{(R_0^{-3} - u^3) du}{(R_0^{-2} - r_S R_0^{-3} - u^2 + u^3 r_S)^{3/2}} \Big|_{r_S=2M=0} \\ &= 2 \int_0^{1/b} \frac{(b^{-3} - u^3)}{(b^{-2} - u^2)^{3/2}} du = 4b^{-1} \end{aligned} \quad (11.16)$$

Finally the deflection angle is in first order

$$\delta\varphi = \Delta\varphi - \pi \approx M \frac{\partial(\Delta\varphi)}{\partial M}\Big|_{M=0} = \frac{2r_0}{b} = \frac{4GM}{c^2 b} \quad (11.17)$$

Note that the impact parameter b gives the shortest distance to M whereas R_0 is the radius at the turning point. In general we have following (11.14) $b > R_0$.

Equ. (11.17) is identical with (11.2). It is the basic formula for **gravitational lensing** which were looking for. In this section we followed Robert M. Wald in a somewhat laborious derivation. However, we have thus avoided any sloppiness which we allowed in lect.1. Furthermore it was shown that (11.2) is really a first order effect.

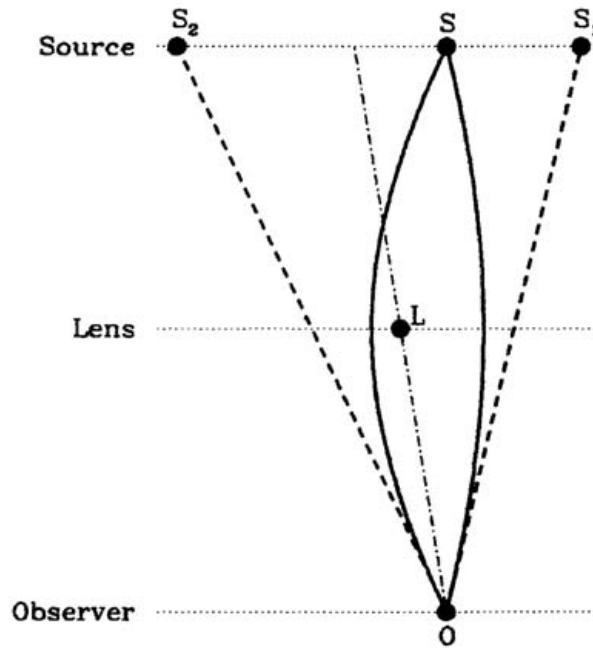


Fig. 11.4. The light rays from the source S are deflected by the lensing point mass L . The observer at O sees two images: S_1 and S_2 .

11.3. Weak lensing, lens equation and Einstein rings.

We assume that the distances to source and lens are very large (Gpc) and the deflection angle small ($\alpha \leq 1$ arc sec). The source is always behind the lens. The deflection results in two rays,

so that the image of the source appears at two different positions: the source is doubled (s. fig.11.4.). We now consider light rays from a source at a distance D_s . They pass a deflecting mass in the lens plane at a distance D_L from us. The distance of the source from the lens plane is D_{LS} . β is the true angular position of the source (without lensing) and η is the true position in the source plane. You note that we have always replaced the sin-function by the angle, e.g. $\sin \beta \approx \beta$ ect.

$$\beta = \frac{\eta}{D_s} \quad (11.18)$$

The ray from the source S passes the deflecting mass L in the lens plane at ξ and an image S_1 appears which we see under the angle θ . We have $\alpha + \beta = \theta$ (s. below) and furthermore

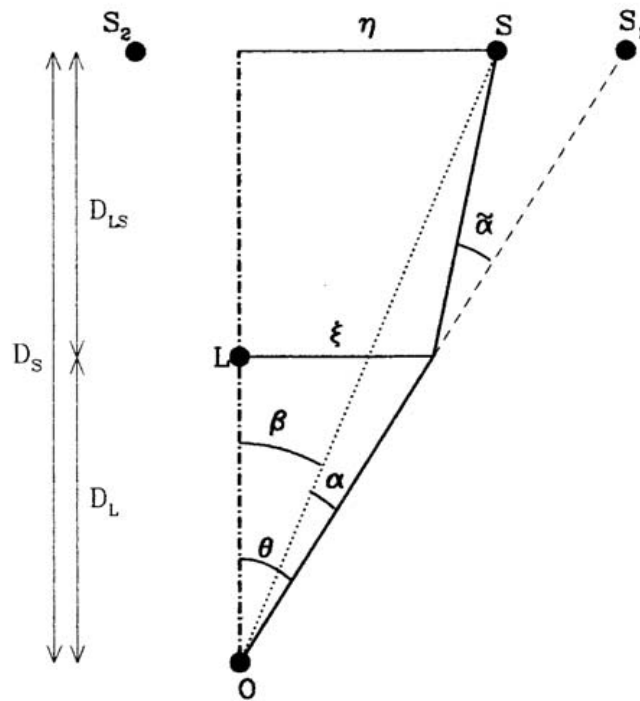


Fig.11.5. Schematic view of the lens geometry. At the right side the curved paths of the light rays are replaced by straight lines. S is the source, L the lensing point mass, S_1 and S_2 are the images of the source. For further details see the text. Credit: J. Wambsganss.

$$\theta = \frac{\xi}{D_L} \quad (11.19)$$

From fig. 11.5 the following relation is evident

$$\theta D_s = \beta D_s + \tilde{\alpha} D_{LS} \quad (11.20)$$

This is the gravitational lens equation. $\tilde{\alpha}$ corresponds to $\delta\varphi$ in fig.11.3. In equ. (11.17) b corresponds to ξ in fig. 11.5 so that we may write

$$\tilde{\alpha}(\xi) = \frac{4GM(\xi)}{c^2} \frac{1}{\xi} \quad (11.21)$$

where $M(\xi)$ is the mass inside a radius ξ . Dividing (11.20) by D_S and using the definition

$$\alpha = \tilde{\alpha} \frac{D_{LS}}{D_S} \quad (11.22)$$

we find with the lens equation

$$\theta = \alpha(\theta) + \beta \quad (11.23)$$

which is a relation between the positions of source (β) and image (α). Actually fig. 11.5 is a 2-dimensional cross section of the lensing geometry. We should take into account that the geometry of lens and source plane needs a 3-dimensional representation. We therefore must view (11.23) as a 2-dim. vector equation and write instead of θ, α and β vector symbols $\theta \rightarrow \vec{\theta}$, $\alpha \rightarrow \vec{\alpha}$ and $\beta \rightarrow \vec{\beta}$. We will now use (11.21), (11.22) and (11.23) to give $\vec{\beta}$ for a point mass

$$\vec{\beta} = \vec{\theta} - \frac{D_{LS}}{D_S} \tilde{\alpha} \frac{4GM}{c^2} \frac{1}{\xi} \quad (11.24)$$

with α

$$\alpha = \frac{D_{LS}}{D_S} \frac{4GM}{c^2} \frac{1}{D_L |\theta|} = \frac{\theta_E^2}{|\theta|^2} \vec{\theta}$$

θ_E is called the **Einstein radius**, a characteristic angle in (11.24)

$$\theta_E^2 = \frac{D_{LS}}{D_S D_L} \frac{4GM}{c^2} \quad (11.25)$$

The Einstein radius defines an angular scale in lensing observations. The second equation, the lens equation of (11.24) is a quadratic equation. We follow P. Schneider, use scaled variables

$$\vec{x} \equiv \frac{\vec{\theta}}{\theta_E} \quad \text{and} \quad \vec{y} \equiv \frac{\beta}{\theta_E} \quad (11.26)$$

and write the lens equation in the following form

$$\vec{y} = \vec{x} - \frac{\vec{x}}{|\vec{x}|^2} \quad (11.27)$$

After multiplication with \vec{x} we find a quadratic equation

$$x^2 - xy - 1 = 0 \quad (11.28)$$

with the solutions

$$|\vec{x}_{1,2}| = \frac{1}{2} \left[|y| \pm \sqrt{|y|^2 + 4} \right] \quad (11.29)$$

From (11.29) we see that lensing by a point mass (lens) has two solutions. The two images are collinear with the lens.

For $\vec{\beta} = 0$ or $\vec{y} = 0$ the source is positioned exactly behind the lens; and in this case $|x| = 1$ or $\theta = \theta_E$. The geometry becomes axially symmetric and an Einstein ring is observed.



Fig. 11.6. Double Einstein ring SDSS J0946+1006 which arises from the light of 3 galaxies. The main lens has a cosmological redshift of $z = 0,222$, the galaxy lensed to the inner ring with an Einstein radius of $1''$, $43 \pm 0,01$ lies at $z = 0,609$. The outer ring has $2''$, $07 \pm 0,02$ at distances corresponding to $z < 6,9$. See fig. 11.8 to convert z in light years. Credit: R. Gavazzi and T. Treu, NASA, ESA and the SLACS Team.

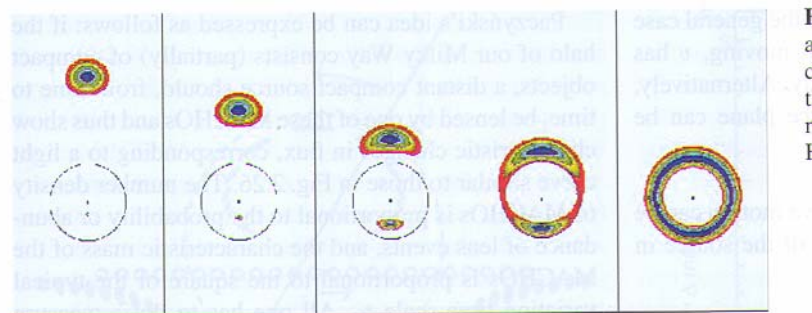


Fig. 11.7. Modelled image of a lensed circular source with a radial brightness profile (indicated by colors). $y = \beta / \theta_E$ decreases from left to right. At the right end of the series $y = 0$ and an Einstein ring is formed. Credit: P. Schneider.

When $|y|$ is small, that is $|y| < 1$, then $\Delta x = |x_1 - x_2| > 2$ since $|x| = \frac{|\theta|}{\theta_E}$

$$\Delta\theta > 2\theta_E \quad (11.30)$$

11.4. Microlensing

Will lensing by stars in our galaxy be observable? With the above derived expressions (s. equ. 11.25) we find (s. P. Schneider)

$$\theta_E = 0,902 \text{ mas} \left(\frac{M}{M_{sol}} \right)^{1/2} \cdot \left(\frac{D_L}{10 \text{ kpc}} \right)^{-1/2} \left(1 - \frac{D_L}{D_S} \right)^{1/2} \quad (11.31)$$

The mas-range (milli-arcsec-range) is outside of the resolution of terrestrial optical telescopes. Even interferometric techniques would not be adequate. However, although we cannot see the splitting of the magnification (i.e. the change in brightness) may well be observable. With the relative motion of source and lens the magnification is time-dependent. The time scale to cross the diameter of an Einstein ring is $t_E = \frac{\theta_E}{\dot{\theta}}$ with

$$\dot{\theta} = \frac{v}{D_L} = 4,22 \text{ mas yr}^{-1} \left(\frac{v}{200 \text{ km/s}} \right) \left(\frac{D_L}{10 \text{ kpc}} \right)^{-1} \quad (11.32)$$

Typical velocities are $v = 100 - 200 \text{ km/s}$. Then t_E is of the order of months and well observable.

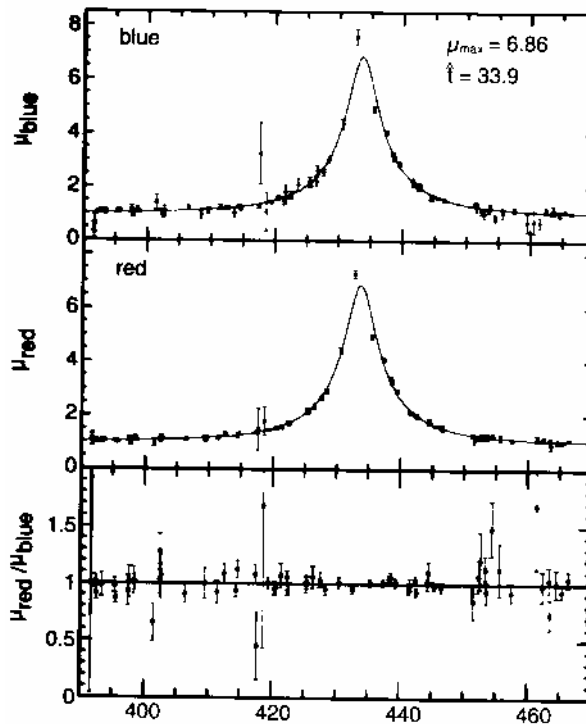


Fig. 11.8. The first observed microlensing event in LMC (see text). The light curves of blue and red light plotted versus time (days from 2 Jan 1992) do not show any difference. This is an important indication that the curves truly exhibit gravitational lensing which should be independent of wavelength. Credit: The MACHO-group and P. Schneider.

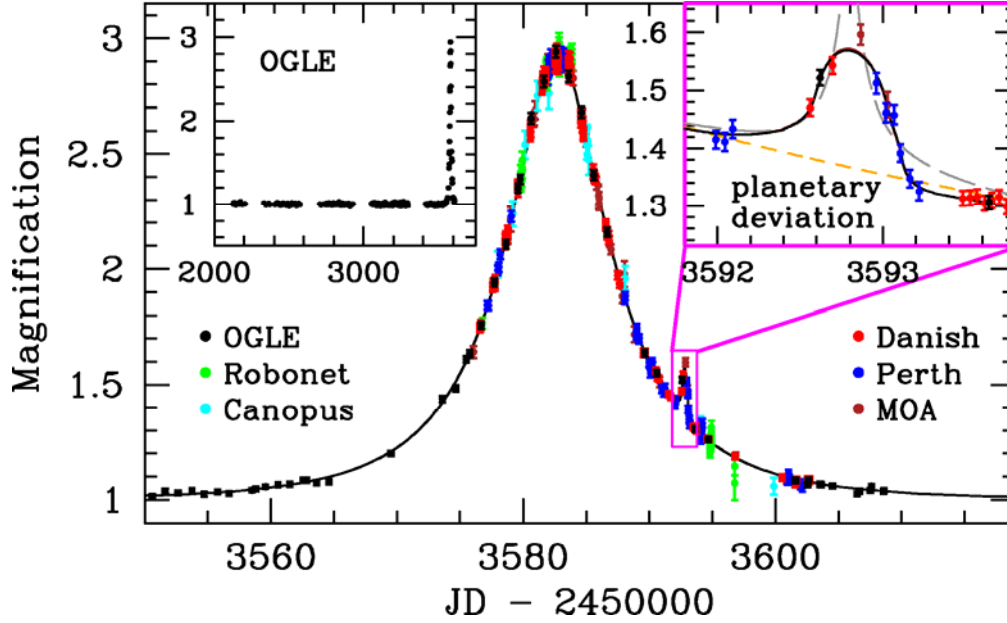


Fig. 11.9. Light curve of a planetary lensing event OGLE 2005-BLG-390. Six groups with various instruments shared in collaboration and thus guaranteed observations around the clock. Credit: The three collaborations PLANET/RoboNet, OGLE, and MOA.

In search for “Dark Matter” between our galaxy and its small neighboring companion the “Large Magellanic Cloud” (distance ca. 50 kpc) two collaborations MACHO and EROS used the micro-lensing effect to find hidden massive objects which would act in the foreground as lenses of LMC stars. During these observations lensing has to be definitely distinguished from intrinsic intensity variations of stars (in the range of a few %). The light curves of lensed objects have a very characteristic shape (fitted by 4 parameters) and are achromatic. In some rare cases the lenses have been identified by their faint spectra as low mass main sequence stars.

11.5. Galaxies acting as gravitational lenses.

The most spectacular observations have been made with galaxies acting as gravitational lenses as we have already seen in fig.11.1, 11.6 and modelled in fig. 11.7. They are only poorly described with point sources. Instead we may use a superposition of point masses (for the stars) or use a smooth mass density. Starting from (11.20) we write for the superposition of m_i masses

$$\vec{\alpha}(\xi) = \sum \frac{4Gm_i}{c^2} \frac{\vec{\xi} - \vec{\xi}_i}{|\vec{\xi} - \vec{\xi}_i|^2} \quad (11.33)$$

We introduce a continuous mass distribution $dm = \Sigma(\xi) d^2 \xi$ with a 2-dimensional mass density $\Sigma(\xi) = \int \rho(\xi, z) dz$ and (11.33) becomes

$$\vec{\alpha}(\xi) = \frac{4G}{c^2} \int d^2 \vec{\xi}' \Sigma(\vec{\xi}') \frac{\vec{\xi} - \vec{\xi}'}{|\vec{\xi} - \vec{\xi}'|^2} \quad (11.34)$$

In order to determine the mass distribution $\Sigma(\vec{\xi})$ from the observational data we would have to solve equ. (11.37) which is an integral equation and therefore a solution is not easily obtained. In a pragmatic approach one uses simple models for the allocation of masses. As a first case we will examine is an **axially symmetric mass distribution**: $\Sigma(\vec{\xi}) = \Sigma(\xi)$. This brings equ. (11.36) in the form

$$\tilde{\alpha} = \frac{4GM(\xi)}{c^2 \xi} \quad (11.35)$$

where the deflection angle is inward directed and $M(\xi)$ ist the mass within the radius ξ . The observed angle is $\alpha = \frac{D_{LS}}{D_S} \tilde{\alpha}$ (s. 11.22), remember also that $\theta = \frac{\xi}{D_L}$ (s. 11.22). Solving for α we get a one-dimensional mapping

$$\alpha = \frac{D_{LS}}{D_S D_L} \frac{4GM(\theta)}{c^2 \theta} = \frac{m(\theta)}{\theta} \quad (11.36)$$

$m(\theta)$ is a normalized mass within the angle θ .

Another favoured model for the mass distribution of a galaxy is the **isothermal sphere**. It takes account of the observation that the mass of a spiral galaxy increases with r which indicates a 3-dimensional density distribution $\rho(r) \propto r^{-2}$ given by an empirical relation

$$\rho(r) = \frac{\sigma_v^2}{2\pi G r^2} \quad (11.37)$$

σ_v^2 is the random mean square of star velocities determined by Doppler shift of spectral lines. (11.37) is motivated by the virial theorem. A projection of the matter on a plane perpendicular to the line of sight gives the surface mass density

$$\Sigma(\xi) = \frac{\sigma_v^2}{2G\xi} \quad (11.38)$$

The projected mass within the radius ξ is then

$$M(\xi) = 2\pi \int_0^\xi d\xi' \xi' \cdot \Sigma(\xi') = \frac{\pi\sigma_v^2 \xi}{G} \quad (11.49)$$

and the deflection angle

$$\tilde{\alpha} = 4\pi \frac{\sigma_v^2}{c^2} \quad (11.40)$$

Using (11.22) we finally find the deflection angle

$$\alpha(\theta) = 4\pi \frac{\sigma_v^2}{c^2} \frac{D_{LS}}{D_S} \equiv \theta_E \quad (11.41)$$



Fig.11.10. The Collision of two galaxy clusters Abell 520 from an X-ray exposure by Chandra (red) and a point by point evaluation of lensing effects (blue). The red colour shows the distribution of “normal” (baryonic) matter, blue is the distribution of dark matter derived from lensing (gravitational shear). Credit: A. Mahdavi Univ. Victoria, NASA, CXC, CFHT)

A typical value for σ_v is about 200 km/s which results in

$$\theta_E = 1'' ,15 \left(\frac{\sigma_v}{200 \text{ km/s}} \right)^2 \frac{D_{LS}}{D_S} \quad (11.42)$$

Note that an Einstein ring for massive galaxies is three orders of magnitude larger than for stars. With θ_E the lens equation may be written

$$\vec{\beta} = \vec{\theta} - \theta_E^2 \cdot \frac{\vec{\theta}}{|\theta|^2} \quad (11.43)$$

We give magnification too but without proof

$$\mu = \frac{|\theta/\theta_E|}{|\theta/\theta_E - 1|} \quad (11.44)$$

Note that the deflection angle is negative $\theta < 0$ and is inward directed. Cosmic distances are usually given as redshift z which is nonlinearly related to the comoving distance $(t_0 - t)c$ in light years. $(t_0 - t)$ is called the “look back time”. The redshift z is linked to the scale factor which describes the changes of distances by the time dependent cosmic expansion (sometimes called Hubble flow)

$$\frac{a(t_0)}{a(t)} = z + 1 \quad (11.45)$$

Here t_0 means the present time and t an arbitrarily earlier time ($t_0 > t$). The plot of fig.11.8 contains the Hubble constant defined as

$$H_0 = \left. \frac{\dot{a}}{a} \right|_{t=t_0} \quad (11.46)$$

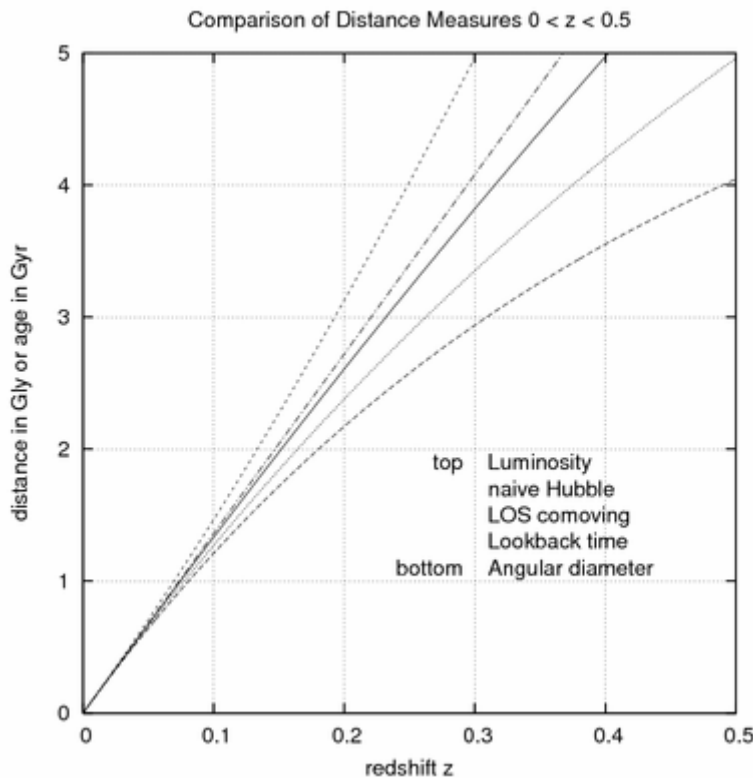
The best present values are

$$H_0 = 74,2 \pm 3,6 \text{ km}\cdot\text{s}^{-1}/\text{Mps (from HST)}$$

and

$$H_0 = 70,5 \pm 1,3 \text{ km}\cdot\text{s}^{-1}/\text{Mps (from WMAP)}$$

We should mention that methods now exist to evaluate images of large arrays of galaxies and determine the lensing effects from the distortion of their shape (gravitational shear). This method enables astrophysicists to determine the distribution of “dark matter” around galaxies and galaxy clusters which is an important contribution to one of the most thrilling unsolved questions of cosmology (s. fig. 11.10):



11.11. Luminosity distance, co-moving distance, „look back time“ and angular distance in units of 10^9 years. $H_0 = 70 \text{ km}\cdot\text{s}^{-1}/\text{Mpc}$ and $\Omega_\Lambda = 0,70$ and $\Omega_M = 0,30$. The diagram allows to convert redshift (z) in “comoving distance” $c(t_0 - t)$ measured by the time the light needed to travel from the distant object to us.

You may know that only 4% of the mass/energy-density of the universe is known matter. About 26% is contributed by “dark matter” of completely unknown nature and about 70% is dark energy. Its density does obviously not change with time. You will hear more about these mysterious properties of the universe in the 12th lecture, our final one.

Let me add a last comment to lensing. There is an obvious similarity between optical and gravitational lensing. Both provide pictures which are linear copies of objects. Take fig. 11.5 and redraw it with slightly changed angles and you will get a representation well know from geometric optics. In the applications, however, there is an important difference between both. In optical imaging we use the image to study the object. On the other hand gravitational lensing is mostly used to study the lens. In some rare cases when astrophysicists study most distant galaxies they appreciate the assistance of an accidental lensing to find the very weak objects. But in most other cases the lenses are used to provide us with unknown mass distributions.

11.6. Problems.

11.6.1. A Galaxy of $M_L = 5 \cdot 10^{12}$ solar masses and a radial extension of $\xi = 100 \text{ kpc}$ at $z = 1,5$ acts as lens for a galaxy at $z = 2,5$. Use equ. 11.42 and make a plausible assumption for σ_v^2 .

Draw a sketch to illustrate the geometry. Note that z and the distances D_S, D_L are nonlinear related. See fig. 11.11 for a conversion $z \Leftrightarrow ct$.

11.6.2. A star in the LMC ($D_S = 50 \text{ kpc}$) acts as source in a micro lensing event. The foreground star is a red dwarf of 0,3 solar mass at a distance of 15 kpc. Assume the two stars are exactly aligned. What would be the angle of the Einstein ring θ_E ?

11.6.3. The relative velocity of the lens is 150 km/s. What is the time t_E in which microlensing can safely be observed? (s. chapter 11.4. Microlensing)

| z | D_A [Mpc] |
|-----|-------------|
| 0.5 | 1241.3 |
| 1.0 | 1628.6 |
| 1.5 | 1720.9 |
| 2.0 | 1702.3 |
| 2.5 | 1641.5 |
| 3.0 | 1566.5 |

Tab. 11.1 The angular distance used in lensing observation versus redshift z .

References

R.M. Wald: General Relativity. Univ. of Chicago Press 1984

J. Wambsganss: Gravitational lensing in astronomy. <http://www.livingreviews.org>. 1998
Amendment 2001

Peter Schneider. Extragalactic astronomy and cosmology. Berlin, Heidelberg, New York